Korean Journal of Nuclear Medicine Technology, Volume 30, Number 2, Article 21, November 2026.
Korean J Nucl Med Technol 2026;30(2):21. https://doi.org/10.12972/kjnmt.2026.30.2.21
pISSN 1229-9901
eISSN 2982-8406

Original article

Evaluation of Regional Radiopharmaceutical Distribution Using a Lead-Collimated Survey Meter in Bone Scintigraphy

Gwang-yeol Park, Radiological Technologist, Sang-Hyeong Kil, Radiological Technologist
Department of Nuclear Medicine, Pusan National University Yangsan Hospital, Yangsan, Korea

Corresponding Author: Sang-Hyeong Kil, Department of Nuclear Medicine, Pusan National University Yangsan Hospital, 20, Geumo-ro, Mulgeum-eup, Yangsan-si, Gyeongsangnam-do, 50612, Republic of Korea. Tel: +82-55-360-1901, E-mail: rlf1007@naver.com

Abstract

Purpose: Handheld survey meters detect photons from both the target region and surrounding tissues, which limits their regional specificity. This study evaluated whether lead collimation strengthens the association between regional survey meter ratios and gamma camera count ratios in patients undergoing ^{99m}Tc-DPD bone scintigraphy. **Materials and Methods**: In this single-center paired-measurement study, 68 adult patients underwent anterior pelvic imaging, followed by survey meter measurements over the bladder, proximal femur, and adjacent soft tissue using an energy-compensated Geiger–Müller survey meter. Measurements were obtained under three conditions: with a 6-mm-thick lead collimator at a detector center-to-skin distance of 10 cm (COL); with a paper replica of identical geometry but without lead shielding (NCOL); and with the detector housing in direct contact with the skin (CONTACT). Bladder-to-soft-tissue ratios (BSRs) and femur-to-soft-tissue ratios (FSRs) were calculated from gamma camera counts and background-corrected dose rates. Spearman correlations were assessed with patient-level bootstrap confidence intervals and Holm correction for six tests. The pre-specified comparison of BSR correlations between the collimated and uncollimated conditions was performed using paired bootstrapping. **Results**: The bladder-to-soft-tissue ratio correlation was strongest under the collimator condition (ρ = 0.597; Holm-adjusted P < 0.001), followed by the skin contact (ρ = 0.416; adjusted P = 0.002) and uncollimated conditions (ρ = 0.299; adjusted P = 0.053). The correlation was significantly higher under the collimator than under the uncollimated condition ($\Delta\rho$ = 0.298; P = 0.022), whereas the collimated and skin-contact conditions difference was not significant (P = 0.188). Femur-to-soft-tissue ratio correlations were not significant under any condition. The association between the collimated survey meter bladder-to-soft-tissue ratio and the gamma camera bladder-to-soft-tissue ratio persisted after adjustment for sex, administered activity, and injection-to-imaging interval (partial ρ = 0.558; P < 0.001). **Conclusion**: Under matched geometry, lead collimation strengthened the association between survey meter and gamma camera bladder-to-soft-tissue ratios. These findings suggest that a lead-collimated survey meter may serve as a supplementary tool for assessing regional radiopharmaceutical distribution in the bladder, potentially supporting pre-imaging assessment and helping reduce the need for repeat bone scintigraphy.

Keywords: ^{99m}Tc-DPD, Bone Scintigraphy, Radiation Survey Meter, Lead Collimator, Regional Activity Distribution

Introduction

Whole-body bone scintigraphy is widely used to evaluate skeletal disorders because tracer uptake reflects regional blood flow and osteoblastic activity. Technetium-99m-labeled dicarboxypropane diphosphonate (^{99m}Tc-DPD) accumulates in bone through adsorption onto hydroxyapatite, whereas unbound tracer is excreted predominantly by the kidneys. Radioactive urine retained in the bladder can obscure adjacent pelvic structures and interfere with image interpretation. Accordingly, bone scintigraphy guidelines recommend adequate hydration and frequent voiding,

Received October 07, 2026 **Revised** October 25, 2026 **Accepted** October 28, 2026

This is an Open Access article distributed under the terms of the Creative Commons CC BY 4.0 license (https://creativecommons.org/licenses/by/4.0/) which permits unrestricted use, distribution, and reproduction in any medium, provided the original work is properly cited.

particularly immediately before imaging[1, 2]. However, a patient's report of having voided does not indicate the amount of residual bladder activity, which depends on renal function, hydration status, time since voiding, and completeness of bladder emptying. A simple method for externally assessing residual bladder activity could therefore support pre-imaging evaluation, provided that its relationship with regional tracer distribution is established.

Handheld radiation survey meters, which are routinely available in nuclear medicine departments, offer a practical means of such external assessment. However, because these instruments measure the radiation field at the detector rather than localizing the anatomical origin of the detected photons, measurements over a specific region may include contributions from adjacent organs and tissues. This limitation is particularly relevant in bone scintigraphy, in which intense bladder activity can contaminate measurements over the nearby proximal femur and soft tissue. Survey meter responses also depend on detector type, photon energy, angle of incidence, and measurement distance[3, 4]; even with energy compensation, variations in the local photon spectrum and scattered radiation may affect the detector response. Improving the regional specificity of external measurements therefore requires standardized measurement geometry and a means of suppressing radiation from outside the target region.

A lead collimator can restrict the photon acceptance angle and reduce contributions from outside the target region[5, 6]. Nautiyal et al. used an ionization-chamber survey meter equipped with a movable focusing collimator to assess organ kinetics and cumulated activity after ^{18}F-FDG administration[7]. Although their findings support the feasibility of collimated external measurements, differences in radionuclide, detector characteristics, and target organs limit their direct applicability to ^{99m}Tc-DPD bone scintigraphy with a Geiger–Müller survey meter. To our knowledge, whether lead collimation improves the assessment of regional tracer distribution under these conditions has not been evaluated clinically. Including the bladder, proximal femur, and adjacent soft tissue, which differ markedly in tracer uptake, allows the performance of this approach to be characterized across a range of target-to-background contrasts.

To quantify regional distribution, bladder and femoral measurements can be normalized to adjacent soft-tissue measurements to yield the bladder-to-soft-tissue ratio (BSR) and femur-to-soft-tissue ratio (FSR), respectively. This within-patient normalization may partially offset variations common to all measured regions, such as those related to administered activity and acquisition timing, but it cannot eliminate region-dependent effects of attenuation, scatter, or detector energy response. Gamma camera region-of-interest (ROI) count ratios can therefore serve as an imaging-based reference for the relative distribution measured with the survey meter. Because gamma camera counts and survey meter dose rates represent different physical quantities, however, the resulting ratios should not be interpreted as interchangeable measures of absolute radioactivity[8].

This study aimed to evaluate the association between regional survey meter dose-rate ratios and the corresponding gamma camera ROI count ratios in patients undergoing ^{99m}Tc-DPD bone scintigraphy. Measurements were performed under three conditions: with a custom-made 6-mm-thick lead collimator (COL); without lead shielding, using a paper replica of identical shape and dimensions to preserve the measurement geometry (NCOL); and with the detector in direct contact with the skin (CONTACT). We hypothesized that lead collimation would strengthen the association between survey meter and gamma camera ratios by reducing contributions from surrounding radiation. This study was designed to provide preliminary evidence on the feasibility of collimated survey meter measurements for assessing regional tracer distribution, particularly in the bladder.

Materials and Methods

1. Study Design and Participants

This single-center, prospective paired-measurement study compared gamma camera image counts with handheld survey meter measurements

obtained in the same patients. Adult patients who underwent ^{99m}Tc-DPD whole-body bone scintigraphy at our institution between March 18 and August 18, 2026, were consecutively enrolled after providing written informed consent. The sample size was not predetermined. A total of 68 patients (43 men and 25 women) with complete gamma camera imaging and survey meter measurements under all three conditions (COL, NCOL, and CONTACT) were included in the final analysis.

2. Radiopharmaceutical Administration and Imaging Time

^{99m}Tc-DPD (370–925 MBq; 10–25 mCi) was administered intravenously according to the institutional clinical protocol, with consideration of body weight and clinical circumstances (median, 555 MBq [15 mCi]). Patients were encouraged to hydrate, and imaging was scheduled 2–3 h after injection. The actual injection-to-imaging interval was recorded for each patient (median, 148 min; range, 113–231 min).

3. Survey Meter and Lead Collimator

An energy-compensated Geiger–Müller (GM) survey meter (RadEye G-10; Thermo Fisher Scientific, Waltham, USA) was used to measure the ambient dose equivalent at 10 mm [H*(10)] in units of μSv/h.

The custom lead collimator was designed to reduce interference from radiation originating outside the target region. It was fabricated from two 3-mm-thick lead sheets. The inner sheet was cut according to a predefined flat pattern and formed into a funnel; the outer sheet, cut slightly larger to accommodate the thickness of the inner layer, was fitted over it, giving a total nominal lead thickness of 6 mm. This thickness, which corresponds to many half-value layers of lead for the 140-keV photons of ^{99m}Tc, was chosen to substantially attenuate photons penetrating the collimator wall.

The funnel had a slant length of 15 cm and tapered toward the patient, with inner diameters of 2 cm at the patient-side aperture and 15 cm at the detector-side opening. This configuration shielded the detector from radiation incident from the superior, inferior, and lateral directions while preferentially admitting photons from the target region through the patient-side aperture. The detector center was positioned 10 cm from the patient-side aperture(Fig. 1, 2).

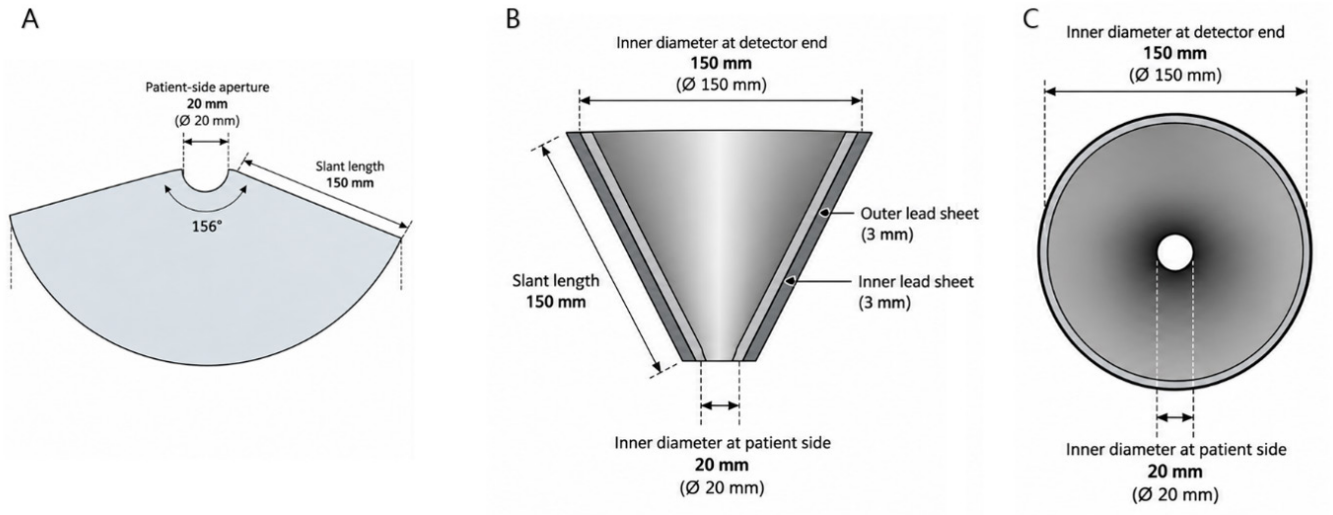


Fig. 1. The illustrations show the design and construction of the custom-made lead collimator. (A) The flat pattern of the inner lead sheet was used to construct the funnel-shaped structure. (B) The cross-sectional schematic illustrates the double-layer lead structure designed to provide radiation shielding. (C) The front view shows the patient-side aperture and the wider detector-side opening.

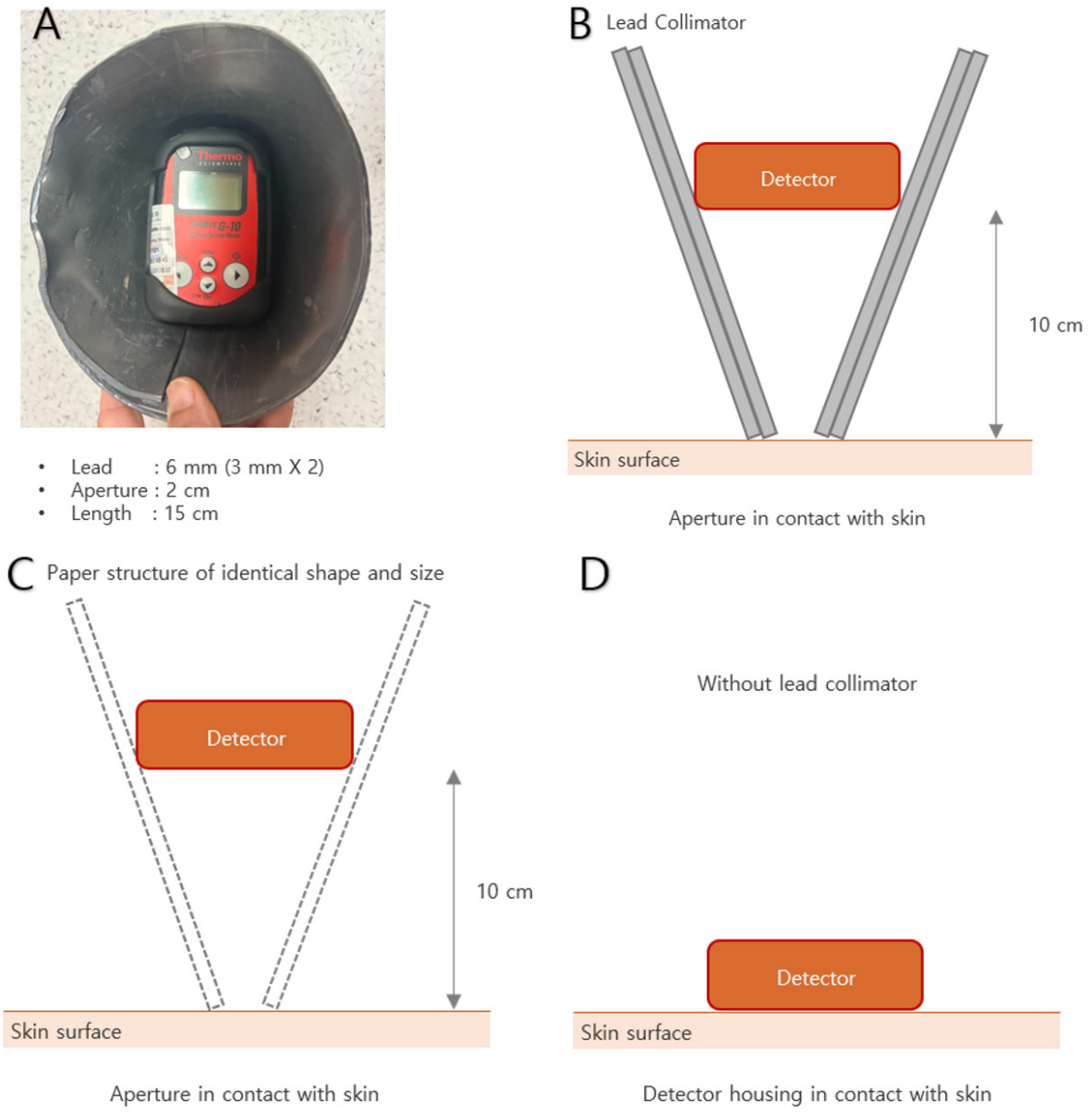


Fig. 2. Custom-made lead collimator and the three survey meter measurement conditions. (A) The funnel-shaped lead collimator was designed to reduce radiation interference from outside the target region. (B) COL condition: the collimator aperture was placed against the patient's skin to obtain directionally restricted measurements. (C) NCOL condition: a paper replica maintained the same measurement geometry without lead shielding. (D) CONTACT condition: the survey meter was placed directly against the skin without a collimator.

4. Gamma Camera Acquisition and ROI Analysis

Images were acquired with a Discovery NM 830 gamma camera (GE HealthCare, Milwaukee, USA) equipped with low-energy high-resolution collimators, using a 256 × 256 matrix and a 15% energy window centered at 140 keV (±7.5%). Anterior images were analyzed because survey meter measurements were obtained from the anterior body surface. After whole-body acquisition, a 2 min anterior pelvic image was acquired without markers. Circular lead markers, 2 cm in diameter to match the collimator aperture, were then placed on the skin over the

bladder, proximal femur, and adjacent soft tissue under visual guidance using the initial pelvic image on the positioning monitor. A second 2 min anterior image was acquired with identical settings while the patient remained in the same position.

The marker image was used to identify the measurement locations, and the corresponding ROIs were transferred to the marker-free image for count analysis(Fig. 3). ROI areas were kept approximately equal (about 100 pixels) to minimize count variation attributable to ROI size, and total counts were extracted from each ROI. Planar ROI counts were not corrected for attenuation, scatter, or detector response.

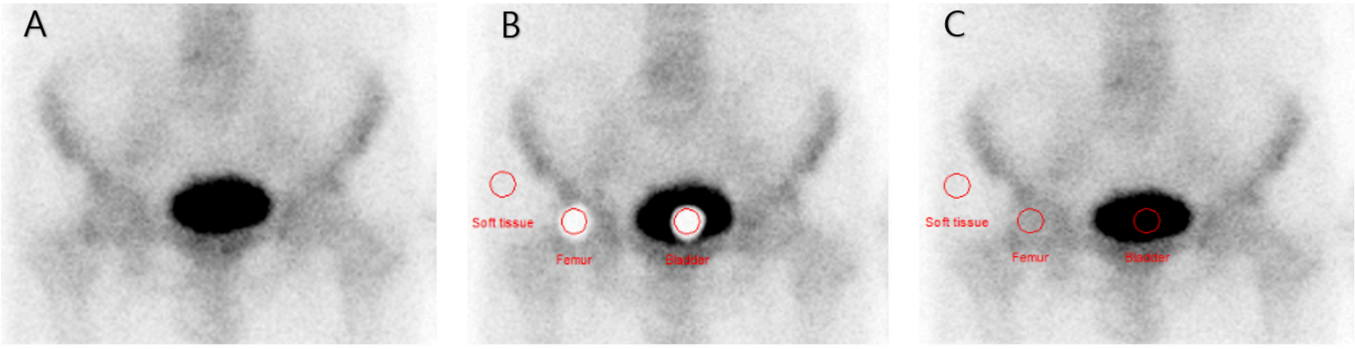


Fig. 3. The anterior gamma camera images illustrate the verification of measurement sites and the delineation of ROIs. (A) The image acquired before lead marker placement was used for ROI count analysis. (B) The image acquired after lead marker placement was used to verify the measurement locations. (C) The ROIs for the bladder, proximal femur, and adjacent soft tissue were delineated on the image acquired before marker placement, using the corresponding marker positions for reference.

5. Survey Meter Measurements and Background Correction

Immediately after gamma camera imaging, the lead markers were removed, with the measurement sites left marked on the skin, and survey meter measurements were performed with the patient in the supine position. Patients did not void between image acquisition and survey meter measurements. Measurements were obtained on the anterior skin surface at the bladder, proximal femur, and adjacent soft-tissue sites corresponding to the gamma camera ROIs. The order of conditions was fixed for all patients (COL, NCOL, then CONTACT), with NCOL measured immediately after COL; the order of measurement sites was also identical across patients and conditions.

COL (collimated): The collimator aperture was placed in contact with the skin, with the detector center 10 cm from the aperture.

NCOL (non-collimated): A paper replica of identical shape and dimensions was placed in contact with the skin, with the detector center 10 cm from the opening, reproducing the COL geometry without lead shielding.

CONTACT (skin contact): The detector housing was placed directly on the skin without a collimator.

At each site and under each condition, the survey meter was held stationary for 20 s before the displayed dose rate was recorded. This was repeated three times, and the mean of the three readings was used as the representative value for each patient, site, and condition. Before patient measurements, the background dose rate was measured in the control room adjacent to the examination room, where contributions from radioactive sources and patients were negligible. Net dose rates were obtained by subtracting the background dose rate from each measured value(Eq. 1) and were used for all ratio calculations.

$$Net\ dose\ rate\left(\frac{\mu Sv}{h}\right) = Measured\ dose\ rate - Background\ dose\ rate \quad \text{Eq. 1}$$

6. Calculation of Regional Relative Ratios

Using adjacent soft tissue as the within-patient reference region, the BSR and FSR were calculated by dividing the gamma camera ROI total counts and the survey meter net dose rates by the corresponding soft-tissue values(Eq. 2, 3).

$$BSR_{GC} = \frac{Bladder\ ROI\ total\ counts}{Soft\ tissue\ ROI\ total\ counts}$$

$$FSR_{GC} = \frac{Proximal\ femur\ ROI\ total\ counts}{Soft\ tissue\ ROI\ total\ counts} \quad \text{Eq. 2}$$

$$BSR_{SM} = \frac{Bladder\ net\ \ dose\ rate}{Soft\ tissue\ net\ dose\ rate}$$

$$FSR_{SM} = \frac{Proximal\ femur\ net\ \ dose\ rate}{Soft\ tissue\ net\ \ dose\ rate} \quad \text{Eq. 3}$$

Survey meter ratios were calculated separately for the COL, NCOL, and CONTACT conditions. All ratios are dimensionless and reflect the combined effects of source activity, attenuation, scatter, and measurement geometry.

7. Study Endpoints

The primary endpoints were the correlations of the COL survey meter BSR and FSR with the corresponding gamma camera count ratios, analyzed separately. The difference in BSR correlation coefficients between the COL and NCOL conditions, which share the same geometry and differ only in lead shielding, was pre-specified as the confirmatory comparison for the collimator effect.

Secondary endpoints were the corresponding correlations under the NCOL and CONTACT conditions, the remaining between-condition comparisons of correlation coefficients, and the correlations between gamma camera ROI total counts and survey meter net dose rates for each region and condition. These analyses assessed association rather than absolute agreement. Exploratory endpoints were the effects of sex, administered activity, and injection-to-imaging interval on the relationship between the gamma camera BSR and the COL survey meter BSR.

8. Statistical Analysis

The data were checked for missing values, duplicate entries, and input errors. Normality was assessed using the Shapiro–Wilk test, and continuous variables are presented as medians and interquartile ranges (IQRs). Because the ratios were not normally distributed, associations were assessed using Spearman rank correlation. The 95% confidence intervals (CIs) were obtained by patient-level bootstrapping with 10,000 resamples (percentile method). Holm correction was applied to the six tests relating gamma camera and survey meter ratios (2 ratios × 3 conditions).

Differences between dependent correlation coefficients ($\Delta\rho$) were assessed by patient-level paired bootstrapping (10,000 resamples), which preserved each patient's measurements across conditions. The pre-specified COL–NCOL BSR comparison was not adjusted for multiplicity; the remaining five comparisons were exploratory, and nominal P values are reported. As a supplementary analysis, simple linear regression of the natural log-transformed survey meter BSR on the natural log-transformed gamma camera BSR was performed for each condition.

Exploratory analyses included Spearman correlations of administered activity and injection-to-imaging interval with the BSR; rank-based partial correlation adjusted for sex, administered activity, and injection-to-imaging interval; and multiple linear regression with the log-transformed COL BSR as the dependent variable and the log-transformed gamma camera BSR and these covariates as independent variables, using heteroscedasticity-consistent (HC3) standard errors. Sex-stratified correlations and leave-one-subject-out sensitivity analyses were also performed. Correlations between ROI total counts and net dose rates were assessed using Spearman analysis. All tests were two-sided, and $P < 0.05$ was considered statistically significant; for the six-test family, significance was based on Holm-adjusted P values. Statistical analyses were performed using IBM SPSS Statistics, version 31.0 (IBM Corp., Armonk, NY, USA).

Results

1. Characteristics of Study Participants

The demographic characteristics and imaging parameters of the 68 patients included in the final analysis are summarized in Table 1. The final dataset contained no missing values or duplicate entries.

Table 1. Baseline characteristics and imaging parameters (n = 68)

Parameter	Value
Sex (male/female)	43 (63.2%) / 25 (36.8%)
Administered activity (MBq)	
Median (IQR)	555 (555-740)
Range	370-925
Time from injection to imaging (min)	
Median (IQR)	148 (126-185)
Range	113-231

*Data are number of patients (%) or median (IQR) and range. IQR, interquartile range.

2. Distribution of Regional Relative Ratios

None of the regional ratios was normally distributed (Shapiro–Wilk test, all $P < 0.001$). The median gamma camera BSR and FSR were 33.18 and 3.78, respectively. Survey meter ratios were lower than the gamma camera ratios under all conditions; they were highest under the COL condition (median BSR, 4.26; FSR, 1.55) and closest to 1 under the NCOL condition (BSR, 1.11; FSR, 1.02)(Table 2).

Table 2. Distribution of regional relative ratios (n = 68)

Equipment and measurement condition	BSR, median (IQR)	FSR, median (IQR)
Gamma camera	33.18 (25.58-49.45)	3.78 (3.21-4.38)
Survey meter, COL	4.26 (2.93-6.06)	1.55 (1.26-1.82)
Survey meter, NCOL	1.11 (1.06-1.16)	1.02 (1.00-1.04)
Survey meter, CONTACT	1.39 (1.21-1.47)	1.24 (1.18-1.29)

*IQR, interquartile range; BSR, bladder-to-soft-tissue ratio; FSR, femur-to-soft-tissue ratio; COL, collimated; NCOL, non-collimated; CONTACT, skin contact.

3. Correlation Between Gamma Camera Count Ratios and Survey Meter Ratios

The BSR correlation was strongest under the COL condition ($\rho = 0.597$; 95% CI, 0.405 to 0.741; Holm-adjusted $P < 0.001$). A significant positive correlation was also observed under the CONTACT condition ($\rho = 0.416$; 95% CI, 0.160 to 0.632; Holm-adjusted $P = 0.002$), whereas the correlation under the NCOL condition was not significant after Holm correction ($\rho = 0.299$; 95% CI, 0.058 to 0.515; Holm-adjusted $P = 0.053$). FSRs were not significantly correlated under any condition (ρ, −0.141 to 0.161; Holm-adjusted $P = 0.566$ for all)(Table 3, Fig. 4).

Table 3. Correlation between gamma camera count ratios and survey meter ratios (n = 68)

Ratio	Condition	Spearman ρ	95% CI	Unadjusted *P*	Holm-adjusted *P*
BSR	COL	0.597	0.405 to 0.741	< 0.001	< 0.001
BSR	NCOL	0.299	0.058 to 0.515	0.013	0.053
BSR	CONTACT	0.416	0.160 to 0.632	< 0.001	0.002
FSR	COL	0.161	−0.064 to 0.375	0.189	0.566
FSR	NCOL	0.075	−0.170 to 0.319	0.544	0.566
FSR	CONTACT	−0.141	−0.374 to 0.107	0.253	0.566

*CIs were calculated by patient-level bootstrapping (10,000 resamples) without correction for multiple testing. Holm correction was applied to the six correlation tests. BSR, bladder-to-soft-tissue ratio; FSR, femur-to-soft-tissue ratio; COL, collimated; NCOL, non-collimated; CONTACT, skin contact; CI, confidence interval.

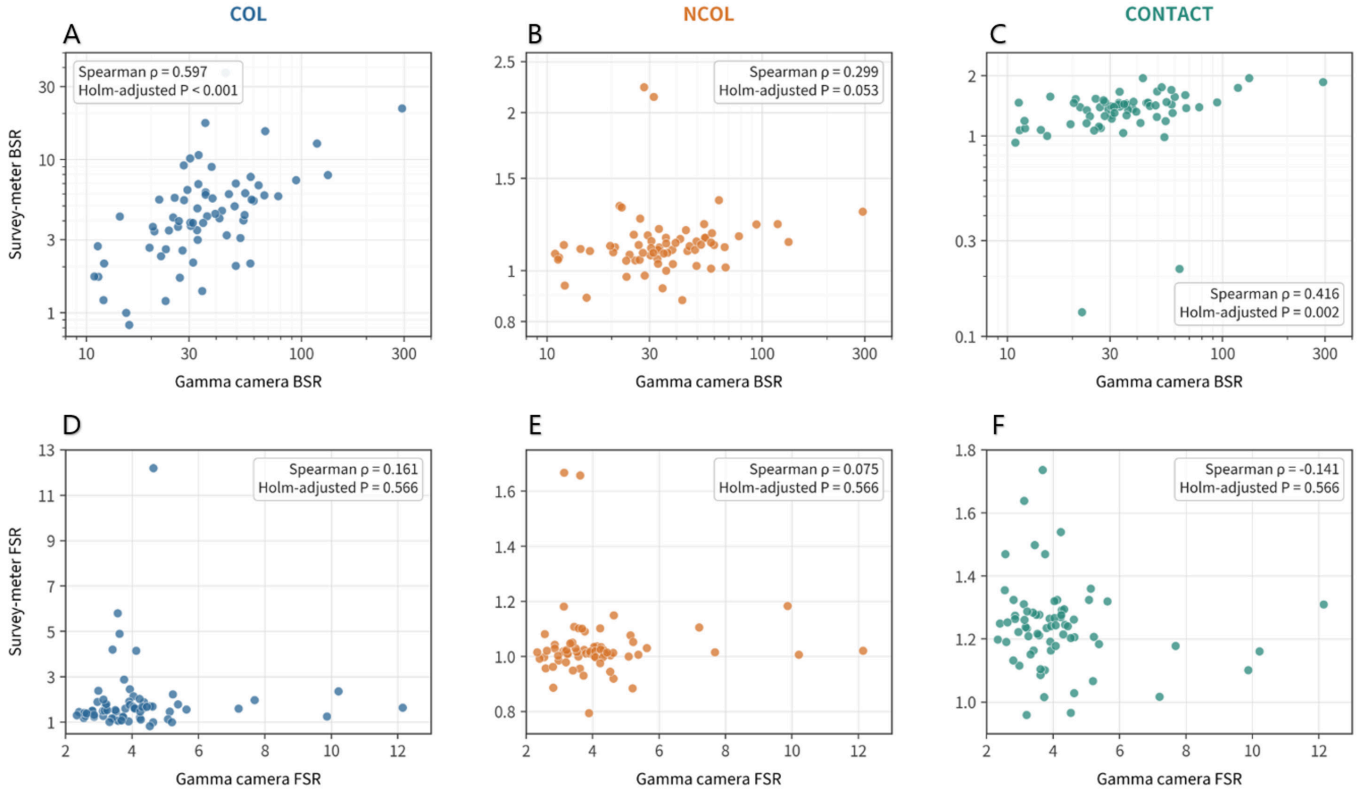


Fig. 4. Scatter plots of gamma camera count ratios versus survey meter ratios. The upper row shows the bladder-to-soft-tissue ratio (BSR) and the lower row the femur-to-soft-tissue ratio (FSR); columns correspond to the collimated (COL), non-collimated (NCOL), and skin-contact (CONTACT) conditions. Each point represents one patient (n = 68). The Spearman correlation coefficient and Holm-adjusted P value (six tests) are shown in each panel.

4. Comparison of Correlation Coefficients According to Lead Collimation

In the pre-specified confirmatory comparison, the BSR correlation was significantly higher under the COL than under the NCOL condition (Δρ = 0.298; 95% CI, 0.039 to 0.552; *P* = 0.022). None of the five exploratory comparisons reached significance, including the COL–CONTACT comparison for BSR (Δρ = 0.181; 95% CI, −0.086 to 0.446; *P* = 0.188)(Table 4).

Table 4. Paired bootstrap comparison of correlation coefficients between measurement conditions (n = 68)

Ratio	Comparison	Δρ	95% CI	*P*
BSR	COL vs. NCOL	0.298	0.039 to 0.552	0.022
BSR	COL vs. CONTACT	0.181	−0.086 to 0.446	0.188
BSR	CONTACT vs. NCOL	0.117	−0.226 to 0.446	0.495
FSR	COL vs. NCOL	0.087	−0.224 to 0.386	0.596
FSR	COL vs. CONTACT	0.302	−0.045 to 0.633	0.090
FSR	CONTACT vs. NCOL	−0.215	−0.512 to 0.079	0.160

*Δρ denotes the difference between the correlation coefficients of the first and second conditions ($\rho_{first} - \rho_{second}$). CIs and *P* values were obtained by patient-level paired bootstrapping (10,000 resamples). Pairwise comparisons were not adjusted for multiple testing; *P* values for exploratory comparisons are nominal. BSR, bladder-to-soft-tissue ratio; FSR, femur-to-soft-tissue ratio; COL, collimated; NCOL, non-collimated; CONTACT, skin contact; CI, confidence interval.

5. Regression Analysis of Log-Transformed Ratios

In simple linear regression of natural log-transformed BSRs, the COL survey meter BSR showed a significant linear relationship with the gamma camera BSR (slope, 0.722; 95% CI, 0.491 to 0.954; $R^2 = 0.371$; $P < 0.001$), whereas no significant relationship was observed under the NCOL (slope, 0.040; $R^2 = 0.028$; $P = 0.171$) or CONTACT condition (slope, 0.145; $R^2 = 0.049$; $P = 0.070$)(Table 5).

Table 5. Simple linear regression analysis of natural log-transformed bladder-to-soft tissue ratios

Measurement condition	Slope (95% CI)	R^2	*P*
COL	0.722 (0.491 to 0.954)	0.371	< 0.001
NCOL	0.040 (−0.018 to 0.099)	0.028	0.171
CONTACT	0.145 (−0.012 to 0.302)	0.049	0.070

*Log-transformed gamma camera BSR was the independent variable and log-transformed survey meter BSR the dependent variable. P values are unadjusted. BSR, bladder-to-soft-tissue ratio; COL, collimated; NCOL, non-collimated; CONTACT, skin contact; CI, confidence interval.

6. Correlation Between Regional ROI Total Counts and Net Dose Rates

Gamma camera ROI total counts correlated positively with survey meter net dose rates in all regions and under all conditions (all unadjusted $P < 0.001$). The highest coefficient was observed for the bladder under the COL condition ($\rho = 0.821$), compared with 0.695 and 0.726 under the NCOL and CONTACT conditions, respectively. Coefficients ranged from 0.663 to 0.676 for the proximal femur and from 0.648 to 0.806 for soft tissue(Table 6).

Table 6. Correlations between regional gamma camera ROI total counts and survey meter net dose rates

Region	Condition	Spearman ρ	Unadjusted *P*
Bladder	COL	0.821	< 0.001
Bladder	NCOL	0.695	< 0.001
Bladder	CONTACT	0.726	< 0.001
Femur	COL	0.663	< 0.001
Femur	NCOL	0.663	< 0.001
Femur	CONTACT	0.676	< 0.001
Soft tissue	COL	0.648	< 0.001
Soft tissue	NCOL	0.803	< 0.001
Soft tissue	CONTACT	0.806	< 0.001

*ROI, region of interest; COL, collimated; NCOL, non-collimated; CONTACT, skin contact.

7. Covariate and Sensitivity Analyses

Administered activity was not significantly correlated with either the gamma camera BSR ($\rho = 0.010$; $P = 0.938$) or the COL survey meter BSR ($\rho = -0.115$; $P = 0.349$). In contrast, the injection-to-imaging interval was negatively correlated with both (gamma camera BSR: $\rho = -0.265$, $P = 0.029$; COL survey meter BSR: $\rho = -0.354$, $P = 0.003$). After adjustment for sex, administered activity, and injection-to-imaging interval, the correlation between the gamma camera BSR and the COL survey meter BSR remained significant (partial Spearman $\rho = 0.558$; $P < 0.001$). In multiple linear regression, the log-transformed gamma camera BSR remained significantly associated with the log-transformed COL survey meter BSR (B = 0.670; 95% CI, 0.471 to 0.868; $P < 0.001$), whereas sex ($P = 0.441$), administered activity ($P = 0.373$), and injection-to-imaging interval ($P = 0.156$) were not significant ($R^2 = 0.418$; adjusted $R^2 = 0.381$). The correlation remained significant in both men (n = 43; $\rho = 0.567$; $P < 0.001$) and women (n = 25; $\rho = 0.672$; $P < 0.001$). In the leave-one-subject-out analysis, ρ ranged from 0.580 to 0.629, consistent with the overall estimate ($\rho = 0.597$)(Table 7).

Table 7. Covariate-adjusted associations and sensitivity analyses of bladder-to-soft-tissue ratios

Analysis	Result	*P*
Correlation with administered activity: gamma camera BSR	$\rho = 0.010$	0.938
Correlation with administered activity: COL survey meter BSR	$\rho = -0.115$	0.349
Correlation with injection-to-imaging interval: gamma camera BSR	$\rho = -0.265$	0.029
Correlation with injection-to-imaging interval: COL survey meter BSR	$\rho = -0.354$	0.003
Partial Spearman correlation (adjusted for sex, activity, interval)	$\rho = 0.558$	< 0.001
Multiple regression: log gamma camera BSR (HC3)	B = 0.670 (95% CI, 0.471 to 0.868); $R^2 = 0.418$, adjusted $R^2 = 0.381$	< 0.001
Sex-stratified correlation: men (n = 43)	$\rho = 0.567$	< 0.001
Sex-stratified correlation: women (n = 25)	$\rho = 0.672$	< 0.001

*BSR, bladder-to-soft-tissue ratio; COL, collimated; CI, confidence interval; HC3, heteroscedasticity-consistent standard errors.

Discussion

In this study, the BSR measured with the collimated survey meter correlated significantly with the gamma camera BSR, whereas the FSR showed no significant correlation under any condition. These findings suggest that the benefit of lead collimation depends on the contrast between the target region and its surroundings. The concept that collimated external measurements can provide information on in vivo distribution has been reported for ^{18}F-FDG[7]; the present study extends this concept to a GM survey meter in ^{99m}Tc-DPD bone scintigraphy. In addition, unlike previous work, this study sought to isolate the effect of the collimator by comparing, within the same patients, COL and NCOL conditions matched for measurement distance and geometry.

In the pre-specified confirmatory comparison, the BSR correlation under the COL condition ($\rho = 0.597$) was significantly higher than that under the NCOL condition ($\rho = 0.299$) ($\Delta\rho = 0.298$; 95% CI, 0.039 to 0.552; $P = 0.022$). Because the two conditions differed not only in lead shielding but also in measurement order, an order effect cannot be excluded. However, because NCOL measurements were obtained immediately after COL measurements, changes in bladder activity over this short interval are unlikely to have substantially altered the ranking of BSRs among patients; the difference therefore most likely reflects the shielding effect.

The collimator effect can be explained by the markedly higher activity in the bladder than in the surrounding soft tissue[1, 2]. Under the NCOL condition, the survey meter BSR was compressed toward 1 (IQR, 1.06–1.16), in stark contrast to the gamma camera BSR (IQR, 25.58–49.45). This dynamic-range compression is attributable to the uncollimated detector receiving photons over a wide solid angle: the intense bladder signal also reaches the detector during soft-tissue measurements, driving the ratio toward 1 and diminishing inter-patient differences. In contrast, the

COL BSR showed a broader distribution (IQR, 2.93–6.06), indicating that the collimator preserved more of the inter-regional difference.

Nevertheless, signal compression persisted partially even with the collimator: the slope of the log–log regression was 0.722, and the median survey meter BSR (4.26) was substantially lower than the median gamma camera BSR (33.18). Possible explanations include the depth-dependent widening of the collimator's field of view, scattered photons, and the fundamental difference between a two-dimensional planar ROI and a three-dimensional detection volume. Because the gamma camera BSR itself contains measurement error, regression dilution may also have contributed to a slope below 1. As the origins of the detected signals were not measured separately, these explanations remain speculative. Thus, although the COL BSR reflects the relative trend of the gamma camera BSR, it cannot be directly converted into the gamma camera value. Moreover, a higher COL BSR indicates only a larger difference in detector response between the bladder and soft tissue; it does not indicate a more accurate measurement of bladder radioactivity.

The CONTACT BSR also correlated significantly with the gamma camera BSR, and its correlation coefficient did not differ significantly from that under the COL condition in the exploratory comparison ($\Delta\rho = 0.181$; $P = 0.188$). Thus, these data establish neither the superiority nor the interchangeability of the two conditions. Signal compression was also evident under the CONTACT condition (IQR, 1.21–1.47); although the rank order was partly preserved, the proportional relationship was largely lost, with the log–log regression explaining only about 5% of the variance ($R^2 = 0.049$). Because the COL and CONTACT conditions also differ in measurement distance and geometry, this comparison reflects differences between two measurement methods rather than the effect of the collimator itself.

No significant FSR correlation was observed under any condition. Because absolute measurements over the proximal femur were significantly correlated between the two instruments, inter-patient variation in absolute values and the relative contrast against soft tissue appear to represent different information. The median gamma camera FSR (3.78) was considerably lower than the BSR, and the survey meter FSR showed an extremely narrow distribution, particularly under the NCOL condition (IQR, 1.00–1.04). In other words, the bone-to-soft-tissue contrast was probably too small for the survey meter to discriminate. Femoral depth and three-dimensional anatomy, photon attenuation and scatter, and detector positioning, all of which influence external radiation detection and quantitative imaging[5, 8], may also have weakened the FSR correlations, as may variability in the soft-tissue reference measurement; however, these factors were not measured individually. Taken together, a lead-collimated survey meter appears better suited to evaluating relative accumulation in regions with markedly high signal, such as the bladder, than to detecting small differences in bone uptake.

The higher correlations observed for absolute measurements than for relative ratios should be interpreted with caution. Absolute values are jointly influenced by patient-specific factors such as administered activity and measurement timing, and therefore do not by themselves reflect the instrument's ability to discriminate distribution between adjacent regions. Normalization to a soft-tissue reference reduces but does not completely eliminate these influences. The absence of a significant correlation between administered activity and BSR is consistent with the intent of normalization. Nevertheless, the soft-tissue measurement itself is affected by physiological distribution and measurement geometry, and when the denominator becomes small after background subtraction, the variability of the ratio can increase. In addition, gamma camera ROI counts are planar indices uncorrected for attenuation, scatter, and detector response, and they include contributions from overlapping tissues along the projection path[8, 9]. The ratios derived from the two instruments should therefore be interpreted not as identical physical quantities but as relative detection responses obtained under their respective conditions.

The injection-to-imaging interval was negatively correlated with both the gamma camera BSR and the COL survey meter BSR. Because this is an inter-patient relationship, it should not be interpreted as indicating that BSR decreases over time within individual patients. Bladder activity is influenced by hydration, renal function, bladder capacity, and voiding status, none of which were assessed in this study. Nonetheless, because the association between the two BSRs remained significant after adjustment for covariates including the injection-to-imaging interval, it cannot be explained by these covariates alone.

These results suggest that fitting a lead collimator to survey meters already available in nuclear medicine departments may enable assessment

of the relative distribution in high-signal regions such as the bladder. However, this study did not evaluate thresholds for determining the need for additional voiding, diagnostic sensitivity and specificity, or improvements in pelvic image quality.

This study has several limitations. First, it was conducted at a single institution in 68 patients undergoing ^{99m}Tc-DPD bone scintigraphy, and the sample size was not determined by a priori power analysis. Second, the spatial response, sensitivity, and angular response of the custom-made collimator were not evaluated using a phantom. Third, the measurement order was fixed (COL, NCOL, then CONTACT); although the interval between conditions was minimized by measuring NCOL immediately after COL, time and order effects cannot be completely ruled out. Fourth, body habitus, target depth, bladder volume, hydration status, renal function, and voiding status were not recorded. Fifth, the results may depend on the specific survey meter (RadEye G-10), collimator, and measurement geometry used. Sixth, measurement repeatability and inter-observer reproducibility were not evaluated; the leave-one-subject-out analysis indicates only that the results were not unduly influenced by any single observation. Seventh, the COL–NCOL comparison for BSR was the only pre-specified confirmatory comparison; the other between-condition comparisons and the covariate and subgroup analyses should be regarded as exploratory. Eighth, a single background value measured in the control room was subtracted under all conditions; because the collimator also shields ambient background radiation, this may have over-corrected the COL measurements, particularly the low soft-tissue dose rates.

Future phantom studies controlling source depth and target-to-background activity ratios should characterize the collimator's spatial response, full width at half maximum (FWHM), sensitivity loss, and recovery of relative ratios, as well as the effects of different aperture sizes and lead thicknesses. Randomization of the measurement order, assessment of repeatability and reproducibility, and comparison with quantitative single-photon emission computed tomography/computed tomography (SPECT/CT) are also needed[9–11]. For clinical application, prospective studies linking pre- and post-voiding measurements to pelvic image quality are essential.

Conclusion

In patients undergoing ^{99m}Tc-DPD bone scintigraphy, the BSR measured with a lead-collimated survey meter correlated moderately with the gamma camera BSR, and this correlation was stronger than that obtained without lead shielding under matched geometry. No such association was observed for FSR under any condition. These findings suggest that a handheld survey meter fitted with a lead collimator may be used to evaluate the relative radiopharmaceutical distribution in regions whose signal substantially exceeds that of the surrounding tissues, such as the bladder, but not to detect subtle differences in bone uptake. These measurements are not quantitative measures of absolute radioactivity and cannot substitute for gamma camera imaging.

References

1. Van den Wyngaert T, Strobel K, Kampen WU, Kuwert T, van der Bruggen W, Mohan HK, et al. The EANM practice guidelines for bone scintigraphy. Eur J Nucl Med Mol Imaging. 2016;43(9):1723-38. DOI: https://doi.org/10.1007/s00259-016-3415-4.
2. Bartel TB, Kuruva M, Gnanasegaran G, Beheshti M, Cohen EJ, Weissman AF, et al. SNMMI Procedure Standard for Bone Scintigraphy 4.0. J Nucl Med Technol. 2018;46(4):398-404. Available at: https://tech.snmjournals.org/content/46/4/398.long
3. Ceklic S, Arandjic D, Zivanovic M, Ciraj-Bjelac O, Lazarevic D. Performance of radiation survey meters in X- and gamma-radiation fields. Radiat Prot Dosimetry. 2014;162(1-2):139-43. DOI: https://doi.org/10.1093/rpd/ncu246.
4. Uhrhan K, Drzezga A, Sudbrock F. The patient as a radioactive source: an intercomparison of survey meters for measurements in nuclear medicine. Radiat Prot Dosimetry. 2014;162(1-2):101-4. DOI: https://doi.org/10.1093/rpd/ncu238.
5. Cherry SR, Sorenson JA, Phelps ME. Physics in Nuclear Medicine. 4th ed. Philadelphia: Elsevier Saunders; 2012.

6. International Atomic Energy Agency. Nuclear Medicine Physics: A Handbook for Teachers and Students. Vienna: International Atomic Energy Agency; 2014.
7. Nautiyal A, Mondal T, Mitra D, Goel A, Dey SK, Kaushik A. A simple and novel approach to study kinetics and estimate radiation doses from internally administered radiopharmaceuticals using an external dose measurement system. Radiat Prot Dosimetry. 2021;196(3-4):141-52. DOI: https://doi.org/10.1093/rpd/ncab141.
8. Bailey DL, Willowson KP. An evidence-based review of quantitative SPECT imaging and potential clinical applications. J Nucl Med. 2013;54(1):83-9. DOI: https://doi.org/10.2967/jnumed.112.111476.
9. Lee WW; K-SPECT Group. Clinical applications of technetium-99m quantitative single-photon emission computed tomography/computed tomography. Nucl Med Mol Imaging. 2019;53(3):172-81. DOI: https://doi.org/10.1007/s13139-019-00588-9.
10. Zanzonico P. Routine quality control of clinical nuclear medicine instrumentation: a brief review. J Nucl Med. 2008;49(7):1114-31. DOI: https://doi.org/10.2967/jnumed.107.050203.
11. De Schepper S, Van den Wyngaert T, Ritt P, Kuwert T. Quantitative SPECT/CT: technique and clinical applications. Molecular Imaging in Oncology-Volume 2: Advanced Solutions to Acquire Disease-Specific Biomarkers-Clinical Applications. 2026;225:619-42. DOI: https://doi.org/10.1007/978-3-032-21415-7_1.